Available online at www.sciencedirect.com
ScienceDirect
ELSEVIER
Materials Science in Semiconductor Processing 9 (2006) 1043–1048
MATERIALS SCIENCE IN SEMICONDUCTOR PROCESSING

XRD and EXAFS studies of HfO_2 crystallisation in SiO_2-HfO_2 films

N.D. Afify[a,*], G. Dalba[a], U. Mahendra Kumar Koppolu[a], C. Armellini[b], Y. Jestin[b], F. Rocca[b]

[a]*Department of Physics, University of Trento, 38050 POVO (Trento), Italy*
[b]*IFN-CNR, Institute for Photonics and Nanotechnologies, Section ITC-Cefsa of Trento, 38050 POVO (Trento), Italy*

Available online 20 November 2006

Abstract

This paper reports a detailed structural study on the nucleation of t-HfO_2 nanocrystals in thin films of $70SiO_2-30HfO_2$ prepared by sol–gel route on v-SiO_2 substrates. Thermal treatment was performed at different temperatures ranging from 900 to 1200 °C for short (30 min) or long (24 h) time periods. Crystallisation and microstructure evolutions were traced by X-ray diffraction (XRD). The local structure around hafnium ions was determined from Hf L_3-edge extended X-ray absorption fine structure (EXAFS) measurements carried out at the BM08-GILDA Beamline of ESRF (France). XRD shows the nucleation of HfO_2 nanocrystals in the tetragonal phase after heat treatment at 1000 °C for 30 min, and a partial phase transformation to the monoclinic phase (m-HfO_2) starts after heat treatment at 1200 °C for 30 min. The lattice parameters as well as the average crystallites size and their distributions were determined as a function of the heat treatment. EXAFS results are in agreement with the XRD ones, with hafnium ions in the film heat treated at 1100 °C for 24 h are present in mixed phases.
© 2006 Elsevier Ltd. All rights reserved.

Keywords: High-*k* materials; SiO_2; HfO_2; XRD; EXAFS; Crystallisation; Thin films

1. Introduction

For many reasons, SiO_2-HfO_2 binary system is one of the best replacements for SiO_2, as the gate dielectric material for standard metal-oxide-semiconductor field effect transistors (MOSFET) [1]. This is mainly due to the fact that the dielectric constant k of HfO_2 is much higher (about six orders of magnitude) than the one of SiO_2. Since thermal stability is a very important issue for high-k materials [2], it is important to have detailed information on their crystallisation history at different processing temperatures.

Pure HfO_2 can exist in three crystalline phases at atmospheric pressures: the monoclinic phase (m-HfO_2) is formed at room temperature, the tetragonal phase (t-HfO_2) is formed at 1720 °C, and the cubic phase (c-HfO_2) is formed at 2600 °C. Above 2800 °C, pure HfO_2 liquifies. At high pressures (typically >3.5 GPa), several orthorhombic phases (o-HfO_2) may be formed [3].

The addition of certain oxides to amorphous HfO_2 and ZrO_2 alters their phase diagrams: the main effects are the modification of the crystallisation temperatures and the appearance of

*Corresponding author.
E-mail address: n_afify@science.unitn.it (N.D. Afify).

1369-8001/$ - see front matter © 2006 Elsevier Ltd. All rights reserved.
doi:10.1016/j.mssp.2006.10.021

high-temperature crystallographic phases (such as cubic or tetragonal) at much lower temperatures. It is known that SiO_2 glass rises the crystallisation temperatures of HfO_2 and ZrO_2 oxides when it is added to them [1]. In Ref. [4], the crystallisation of $(1-x)SiO_2-xHfO_2$ (with $x = 30$, 50, 70, and 90 mol%) powders prepared by sol–gel route has been studied using differential scanning calorimetry (DSC), room- and high-temperature X-ray diffraction (XRD and HTXRD), scanning electron microscopy (SEM), energy dispersive spectroscopy (EDS), and high-resolution transmission electron microscopy (HRTEM). In that work, it has been reported that the system with the composition $70SiO_2-30HfO_2$ crystallises into the t-HfO_2 phase at 1060 °C, with an average crystallite size of 25 Å. The authors in Ref. [5] have studied the crystallisation of $xLa_2O_3-(1-x)HfO_2$ (with $x = 4$, 9, 22, 32, and 51 at%) system prepared in bulk format by precipitation from aqueous solutions. They have shown that for low La_2O_3 concentrations (4 and 9 at%) the t-HfO_2 phase was present, while for high La_2O_3 concentrations (22, 32, and 51 at%) the crystallised phase was c-HfO_2. Neumayer et al. [6] have followed the crystallisation in $(100-x)SiO_2-xHfO_2$ (with $x = 15\%$, 25%, 50%, and 75%) thin films prepared by chemical solution deposition, and deposited on silicon substrates by spin-coating technique. They have reported the appearance of the t-HfO_2 phase in the composition $85SiO_2-15HfO_2$ after heat treatment at 1000 °C for 30 min. This tetragonal phase transforms to the m-HfO_2 phase after thermal annealing at 1200 °C for 60 min. Although the formation of tetragonal phase at relatively low temperatures in the case of ZrO_2 has been deeply studied, we have found few reports in the case of HfO_2, where the structure (e.g. lattice parameters) and microstructure (e.g. crystallite size) were rarely detailed.

In a previous article [7], we have presented extended X-ray absorption fine structure (EXAFS) results on Er^{3+}-doped SiO_2-HfO_2 thin films with HfO_2 concentration ranging from 10 to 50 mol% and Er^{3+} concentration ranging from 0.3 to 0.5 mol%. It has been demonstrated that the system remains amorphous up to heat treatment at 900 °C for 5 min, independently on HfO_2 and Er^{3+} contents [7,8].

In the present paper, we report detailed results on the hafnium local structure, and on the crystallisation as well as the microstructure of HfO_2 in $70SiO_2-30HfO_2$ thin films heat treated at different temperatures for short and long time periods. Crystallisation and microstructure have been followed by XRD; local structure around hafnium ions has been investigated by EXAFS.

2. Experimental details

SiO_2–HfO_2 solution was prepared by sol–gel route, and deposited on v-SiO_2 substrates using the dip-coating method. The starting solution was obtained by mixing tetraethylorthosilicate (TEOS), ethanol (EtOH), deionised water (H_2O), and hydrochloric acid (HCl) as a catalyst. The TEOS:HCl:H_2O molar ratio was of 1:0.01:2.0. This solution was prehydrolysed for 1 h at 65 °C. An ethanolic colloidal suspension was prepared using hafnium oxychloride ($HfOCl_2 \cdot 8H_2O$) as a precursor for hafnium. The two solutions were mixed in the molar ratio 70:30, respectively, so to have a solution with 30 mol% HfO_2 and 70 mol% SiO_2. The resulting mixture was left under stirring for 16 h at room temperature. This solution was then dip-coated on many clean v-SiO_2 substrates, with a dipping rate of 40 mm/min [9]. After each dipping cycle, heat treatment at 900 °C for 55 s in air was carried out. After each 10 dips, the film was heat treated at 900 °C for 2 min. Finally, the thin films were further thermally treated in air at 900 °C for 5 min, so as to achieve a full densification of the films, as it was verified by Raman spectroscopy. In this way, a set of many identical thin films were obtained. Each film was successively heat treated for one time only at a temperature between 900 and 1200 °C. At each temperature two films were treated: one for short (30 min) and the second for long (24 h) time periods. The final thickness of the $70SiO_2-30HfO_2$ films resulted as less than 1 μm (the total number of dips for each film was 20). The films were cracks-free and of high optical quality. The investigated samples are here named as follows: 900S, 900L, 1000S, 1000L, 1100S, 1100L, and 1200S (number and letter stand for heat treatment temperature and time period, respectively (S and L mean 30 min and 24 h, respectively)).

XRD experiments were carried out using X'Pert PRO diffractometer equipped with Cu target as a radiation source. Since the thickness of the measured thin films was small, the grazing incidence X-ray diffraction (GIXRD) set-up, with an incidence angle of 1.5°, was employed. The Rietveld refinement [10,11] was carried out using the general structure analysis system (GSAS) code [12]. The

average crystallites size and their distributions were determined from XRD data, assuming log-normal distributions of spherical crystallites [13].

EXAFS measurements were carried out at the BM08-GILDA Beamline of ESRF (France), where also our previous experiments on rare-earths-doped SiO_2 glasses were done [14,15]. Hf L_3-edge EXAFS spectra were collected at room temperature in fluorescence mode. Due to time limitation, EXAFS measurements were carried out only on the two samples 900S and 1100L. Polycrystalline m-HfO_2 was measured in transmission mode, as a reference compound for EXAFS data modelling. The X-ray absorption spectra were analysed using the EXTRA code [16] to obtain the local structure-dependent part $\chi(k)$. To extract structural parameters (coordination number N, average interatomic distance R, and Debye–Waller disorder factor σ^2), the $k^2\chi(k)$ EXAFS signals were modelled using the EDA code [17,18]. The backscattering functions, required for EXAFS data fitting, were theoretically calculated using the FEFF8 code [19,20], starting from the crystal structure of m-HfO_2. The calculated functions were tested and optimised against the experimentally measured reference compound.

3. Results and discussion

XRD patterns of the different samples are reported in Fig. 1a (dotted lines). All the spectra contain a contribution from the amorphous film. In particular, the hump centred at $2\theta \approx 21^\circ$ is present for all samples, as a typical feature of SiO_2 glass (70 mol% of the film). The sample 900L is fully amorphous, as it is seen by XRD. It is evident that the crystallisation of $70SiO_2-30HfO_2$ film starts after heat treatment at about 1000 °C for 30 min (sample 1000S). The observed Bragg peaks however are very broad, revealing the nanosize nature of the formed crystallites.

To attribute the crystalline phase(s), the positions of Bragg peaks were compared to the Inorganic Crystal Structure Database (ICSD). These peaks correspond to those calculated from the ICSD card No. 85322 (shown by blue lines in Fig. 1a). This card belongs to the metastable t-ZrO_2 phase (the card for the metastable t-HfO_2 phase is not yet present in database). Since HfO_2 and ZrO_2 have the same structures [21], it turns out that the $70SiO_2$–$30HfO_2$ film crystallises into the metastable t-HfO_2 phase. After heat treating of the thin film at 1200 °C for 30 min, a new crystalline phase starts to appear, the main peak of which is centred at $2\theta \approx 28.5^\circ$ (indicated by the $*$ sign in Fig. 1a). This phase corresponds to the m-HfO_2 symmetry (ICSD card No. 27313).

The XRD patterns calculated from the Rietveld best-fit results are reported in Fig. 1a (continuous lines). All spectra were fitted to a single phase (t-HfO_2), except for the sample 1200S, where the m-HfO_2 phase was also included. For the t-HfO_2 phase, the lattice parameters a and c, and the tetragonality c/a are reported in Fig. 1b. The lattice parameter error bars are the numerical values given

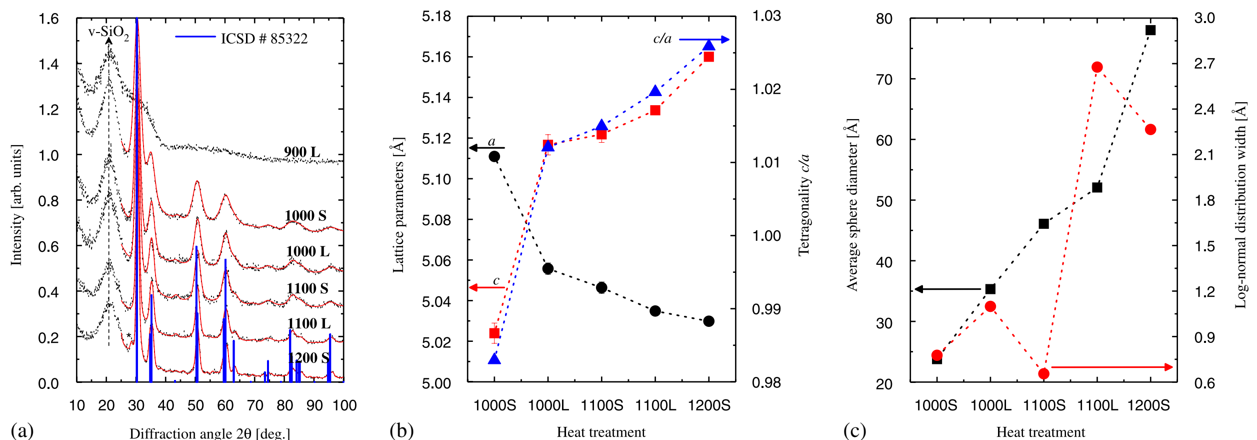

Fig. 1. X-ray diffraction results on $70SiO_2$–$30HfO_2$ thin film at different heat treatments: (a) experimental (dotted lines) and Rietveld-refined (continuous lines) X-ray diffraction patterns. The vertical blue lines represent the unbroadened X-ray diffraction peaks calculated from t-ZrO_2 structure (ICSD card No. 85322). The $*$ sign indicates the major peak of the m-HfO_2 phase. (b) Lattice parameters a (◯) and c (■), and tetragonality c/a (▲), and (c) average crystallites diameter (■) and log-normal distribution width (◯) of the t-HfO_2 phase. The dotted lines in panels (b) and (c) are plotted to guide the eye.

by GSAS code correlation matrix. The effect of heat treatment is illustrated in Fig. 1b as unit cell contraction in the *a* direction, and expansion in the *c* direction. This deformation of the unit cell is a typical behaviour of the metastable tetragonal phase [22], which is seen as a distortion from the ideal fluorite structure (i.e. c-HfO_2) [23]. More significant is the tetragonality c/a trend. It increases on heat treatment, indicating an increasing stability of the t-HfO_2 phase. For tetragonal symmetry, the tetragonality ratio should lie between 1.0 and 1.02 [22]. For the sample 1200S, it appears that $c/a > 1.02$, which is higher than the upper limit [23]. This explains the initiation of transformation to the m-HfO_2 phase. For the sample 1000S, the tetragonality is less than 1.0. This result may be due to large uncertainties on the lattice parameters, because the Bragg peaks of this sample are severely broad. However, we should mention that in Ref. [23], a t-HfO_2 phase with c/a equalling 1.0 has been reported. Moreover, our EXAFS results on the same sample, but doped with 1 mol% Er^{3+} [24] and whose XRD pattern is identical to the one shown by the sample 1000S, have shown that the HfO_2 phase in this case is also tetragonal.

Fig. 1c reports another important result: the mean crystallites diameter and their log-normal distribution width, as functions in heat treatment. From this figure, it can be seen that the mean crystallites size systematically increases on heat treatment, with an abrupt change between the samples 1100L and 1200S. From this analysis, the critical crystallites size, above which the t → m phase transformation starts [22], is determined at about 50 Å.

It is also important to compare the crystallites size distribution widths for samples heat treated at the same temperatures but for different time periods. From Fig. 1c, it appears that heat treatment for short time period (30 min) gives rise to narrower distribution of crystallites size, and therefore more homogenous media of nanocrystals.

Fig. 2 reports the experimental (dotted lines) and best-fit calculated (continuous lines) Fourier transforms of $k^2\chi(k)$ EXAFS signals of the samples 900S and 1100L. The coordination numbers N, average interatomic distances R, and Debye–Waller disorder factors σ^2 of the first and second coordination shells around hafnium ions, as were obtained from the EXAFS data modelling, are complied in Table 1. In both figure and table, the corresponding results for

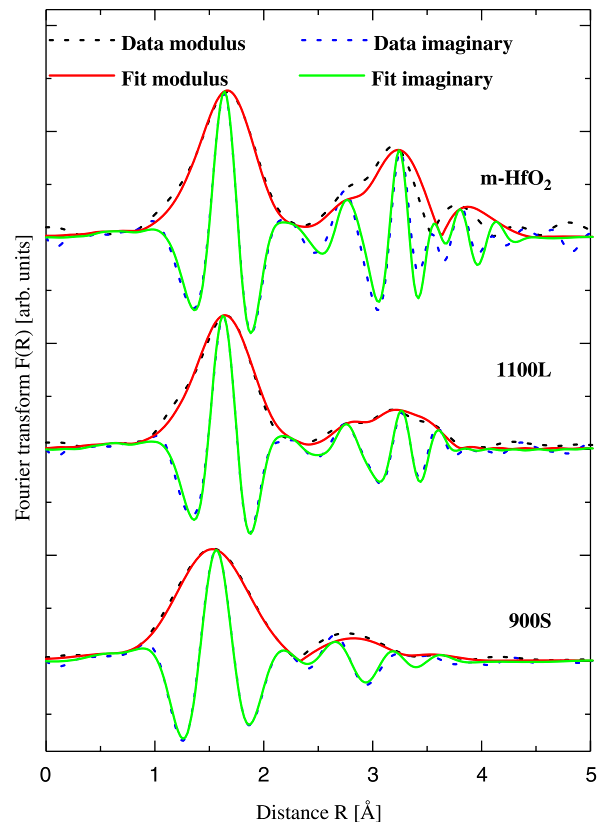

Fig. 2. Experimental (dotted lines) and best-fit calculated (continuous lines) Fourier transforms of $k^2\chi(k)$ EXAFS signals of $70SiO_2-30HfO_2$ thin film heat treated at 900 °C for 30 min (sample 900S) and 1100 °C for 24 h (sample 1100L), compared to the ones of m-HfO_2 reference compound.

the m-HfO_2 reference material are also present for comparison.

As it is expected, the Fourier transform for the sample m-HfO_2 is more structured, due to the crystalline (ordered) environment around hafnium ions. In this sample, three coordination shells are detected around hafnium by EXAFS: Hf–O, Hf–Hf, and another Hf–Hf at farther distances. The Fourier transform for the sample 900S is typical for an amorphous material. In fact, beyond the first coordination shell, only a little broad contribution from the external shells can be seen. This agrees with XRD data, which have demonstrated the pure amorphous nature of HfO_2 in this sample. According to EXAFS data modelling, only two coordination shells are detected around hafnium ions in this case. The first is related to oxygen, and the second is related to hafnium atoms. The effect of crystallinity on the hafnium local environment is documented in Fig. 2 for the sample 1100L: the contributions from

Table 1
Structural parameters of the first (Hf–O) and second (Hf–Hf) coordination shells around hafnium in the samples 900S, 1100L, and m-HfO_2, as were obtained from EXAFS data modelling

Sample		900S	1100L	m-HfO_2
First coordination shell (Hf–O)	N (atom)	5.4 (3)	6.1 (1)	7 (fixed)
	R (Å)	2.087 (2)	2.126 (2)	2.129 (1)
	σ^2 (Å^2)	0.015 (1)	0.010 (4)	0.01047 (2)
Second coordination shell (Hf–Hf)	N (atom)	8.2 (2)	4 (1)	7 (fixed)
	R (Å)	3.361 (1)	3.46 (1)	3.435 (1)
	σ^2 (Å^2)	0.0227 (1)	0.006 (1)	0.0064 (1)

N, R, and σ^2 are the coordination numbers, average interatomic distances, and Debye–Waller disorder factors respectively. Numbers in parenthesis are the estimated uncertainty on last digit taking into account different best-fit parameters.

external shells are more structured in comparison with those in the sample 900S, revealing the evolution towards a more ordered local environment around hafnium. As in the samples 900S and m-HfO_2, the second coordination shell around hafnium was attributed to Hf atoms.

Now we discuss the EXAFS quantitative results (see Table 1). For the sample m-HfO_2, the coordination number of the second coordination shell has been fixed during the fit, to avoid a correlation with the coordination number of the third coordination shell, which is also composed of hafnium atoms (not reported in the table). The EXAFS first and second coordination shell distances (2.129 and 3.435 Å) are generally in agreement with those (2.144 and 3.437 Å) derived from the Rietveld refinement results carried out by the present authors on XRD data from the same sample [24]. The EXAFS distance for the first coordination shell is shorter than the XRD one. This difference, however, may be due to the approximation of seven oxygen atoms, that are crystallographically located at seven different distances, to a single Gaussian distribution of distances in EXAFS data fitting. The EXAFS structural parameters for the sample 900S are in agreement with those obtained on densified ZrO_2 glass prepared by sol–gel route [22], which once again confirms the amorphous nature of this sample, as it has been already shown by XRD data. As for the sample 1100L, it might be seen in Table 1 that the interatomic distances are longer than those of the sample 900S with a tendency towards typical distances of m-HfO_2. However, this should not be interpreted as a simple presence of HfO_2 in the monoclinic structure. In fact, taking EXAFS results on a full set of heat treatments (but the samples were containing 1 mol% Er^{3+}) [24] into account, the structural parameters of the sample 1100L lie somewhere between those of the amorphous sample and those of a sample crystallised mainly in the t-HfO_2 phase. Anyway, for this sample EXAFS sees an average local structure around hafnium in both amorphous, tetragonal as well as possible traces of monoclinic HfO_2 phases.

4. Conclusions

In this paper, crystallisation and microstructure of HfO_2 in $70SiO_2-30HfO_2$ thin films, prepared by sol–gel route and deposited by dip-coating method, have been described by XRD and EXAFS techniques. It has been shown that it is possible to maintain the film fully amorphous at least up to 900 °C, even after long heat treatment. A short thermal treatment at 1000 °C is sufficient to start the partial crystallisation of HfO_2 in tetragonal phase. The dimension of the obtained nanocrystals increases with temperature and time of heat treatment. The homogeneity of nanocrystals size can be controlled by reducing the time of heat treatment. Partial transformation to the m-HfO_2 phase starts after heat treatment at about 1200 °C for 30 min. EXAFS data, being sensitive to both amorphous and crystalline regions, indicate for the film heat treated at 1100 °C for 24 h that a part of HfO_2 is still in amorphous phase.

It is widely accepted that, for high-k applications it is better to have the material amorphous at different processing temperatures. Density functional theory (DFT) calculations on crystalline HfO_2 showed strong dependencies of the dielectric properties on the type of crystalline phase, and proposed the tetragonal phase as the most useful one [21]. In the present work, we have shown the

possibility of obtaining the nanocrystalline t-HfO_2 phase with a controlled microstructure up to heat treatment of 1100 °C for 24 h. It turns out that some experimental work on the dielectric properties of such nanocrystalline SiO_2-HfO_2 films at different processing temperatures is required, in order to explore their potential as high-*k* gate materials.

Acknowledgements

The financial supports by ESRF (France), INFM (Italy), and PAT-FAPVU 2004–2006 are acknowledged. The authors are grateful to Dr. Fabrizio Bardelli of the BM08-GILDA Beamline of ESRF (France), for his kind assistance during the EXAFS measurements. Nasser Afify wishes to thank Dr. Alexei Kuzmin for very useful discussions during the EXAFS data analysis.

References

[1] Robertson J. Rep Prog Phys 2006;69:327.
[2] Zhao C, Roebben G, Heyns M, der Biest OV. Key Eng Mater 2002;206–213:1285.
[3] Wang J, Li H, Steven R. J Mater Sci 1992;27:5397.
[4] Ushakov SV, Navrotsky A, Yang Y, Stemmer S, Kukli K, Ritala M, et al. Phys Status Solidi B 2004;241:2268.
[5] Ushakov SV, Brown C, Navrotsky A. J Mater Res 2004;19:693.
[6] Neumayer DA, Cartier E. J Appl Phys 2001;90:1801.
[7] Afify ND, Grisenti R, Dalba G, Armellini C, Ferrari M, Larcheri S, et al. Opt Mater 2006;28:864.
[8] Gonçalves RR, Carturan G, Montagna M, Ferrari M, Zampedri L, Pelli S, et al. Opt Mater 2004;25:131.
[9] Gonçalves RR, Carturan G, Zampedri L, Ferrari M, Montagna M, Chiasera A, et al. Appl Phys Lett 2002;81:28.
[10] Rietveld HM. Acta Crystallogr 1967;22:151.
[11] Rietveld HM. J Appl Crystallogr 1969;2:65.
[12] Larson AC, Von Dreele RB. Los Alamos National Laboratory Report LAUR, 2000. p. 86.
[13] Langford JI, Louër D, Scardi P. J Appl Crystallogr 2000;33:964.
[14] Rocca F, Ferrari M, Kuzmin A, Daldosso N, Duverger C, Monti F. J Non-Cryst Solids 2001;293:112.
[15] Rocca F, Armellini C, Ferrari M, Dalba G, Diab N, Kuzmin A, et al. J Sol–Gel Sci Technol 2003;26:267.
[16] Fornasini P, Rocca F. EXTRA code for EXAFS analysis, University of Trento, 1998.
[17] Kuzmin A. Physica B 1995;208–209:175.
[18] Kuzmin A, Purans J. J Phys C 2000;12:1959.
[19] Rehr JJ, de Leon JM, Zabinsky S, Albers R. J Am Chem Soc 1991;113:5135.
[20] Mustre de Leon J, Rehr J, Zabinsky S, Albers R. Phys Rev B 1991;44:4146.
[21] Zhao X, Vanderbilt D. Phys Rev B 2002;65:233106.
[22] Southon P, PhD thesis, University of Technology, Sydney, 2000, ⟨ http://adt.lib.uts.edu.au/public/⟩.
[23] Fujimori H, Yashima M, Sasaki S, Kakihana M, Mori T, Tanaka M, et al. Chem Phys Lett 2001;346:217.
[24] Afify ND, Ph.D. thesis, University of Trento, Trento, Italy, 2005.